ISSN 0027-1349, Moscow University Physics Bulletin, 2024, Vol. 79, Suppl. 2, pp. S798–S806. © Allerton Press, Inc., 2024.

Forecasting the State of the Earth's Magnetosphere Using a Special Algorithm for Working with Multidimensional Time Series

R. D. Vladimirov[1]*, V. R. Shirokiy[1], O. G. Barinov[1], S. A. Dolenko[1], and I. N. Myagkova[1]

[1] *Skobeltsyn Institute of Nuclear Physics, Lomonosov Moscow State University, Moscow, 119991 Russia*

Received October 1, 2024; revised October 10, 2024; accepted October 20, 2024

Abstract—This study is devoted to the adaptation and application of a special multistage algorithm based on machine learning methods, developed for the analysis of multidimensional time series in solving problems of forecasting certain events and identifying their precursors—phenomena represented by an unknown combination of parameter values describing an object. In addition to forecasting events, the algorithm can be used to forecast the values of continuous quantities. In this study, we compare the results of application of this algorithm in forecasting of three physical quantities characterizing the state of the magnetosphere of the Earth—two geomagnetic indexes (Dst and Kp) and the flux of relativistic electrons ($E > 2$ MeV) in geostationary orbit.

Keywords: geomagnetic disturbances, Dst-index, Kp-index, electron flux, time series forecasting, machine learning, gradient boosting, linear regression, dimensionality reduction, feature importance

DOI: 10.3103/S0027134924702266

1. INTRODUCTION

1.1. Space Weather

Forecasting the state of the Earth's magnetosphere changing under the influence of space weather is one of the most important applied tasks of modern physics of solar-terrestrial relations of space weather factors, the role of which will increase with the further development of digitalization both on Earth and in space [1–3].

By the state of the Earth's magnetosphere we understand primarily the radiation state of near-Earth space (NES), as well as the level of geomagnetic field perturbation, or geomagnetic disturbances. The radiation state of the NES is largely determined by the fluxes of relativistic and sub-relativistic electrons of the Earth's outer radiation belt (ERB), especially in the absence of solar events. These fluxes are the subject of forecasting. This task is extremely urgent because, despite the fact that the radiation belts were discovered at the dawn of the space age, and there are numerous empirical and numerical models of electron acceleration in the Earth's magnetosphere, e.g., [4, 5] and references therein, there is still no generally accepted theory explaining the formation and dynamics of the outer ERB. It is known experimentally that the outer radiation belt can change strongly under the action of changing factors of the space environment—the interplanetary magnetic field (IMF) and its components, as well as solar wind (SW). Therefore, in order to ensure radiation safety, the task of predicting the relativistic electron (RE) flux in the outer ERB is set.

The task of predicting the RE flux in the outer ERB is also very relevant because the flux of RE (called "killer electrons" in the English-language scientific literature), can negatively affect the operation of spacecraft, damaging onboard microcircuits (e.g., [6]). Moreover, with further reduction of the size of electronics onboard spacecraft, the negative impact of RE fluxes will increase.

A parallel problem similar in solution methods is the prediction of the amplitude of geomagnetic disturbances, which are usually characterized by geomagnetic indices—Kp and Dst. It is also of great practical interest because magnetic storms can cause malfunctions in radio communications, pipelines, power lines, and electric grids, and can also cause human health problems [7–10]. In addition, geomagnetic disturbances affect the radiation situation in the NES, since it is known from experiments that after about half of magnetic storms, the relativistic electron flux of the Earth's outer radiation belt increases by an order of magnitude or more [11, 12].

*E-mail: vladimirov@srd.sinp.msu.ru

One of the most widespread geomagnetic indices is the Dst-index (abbreviation from disturbance storm-time), the forecasting of which is our task. This index was introduced by M. Sugiura in 1964 in [13]. This index is considered as a measure of the geomagnetic field change due to the influence of the ring current, which occurs in the Earth's magnetosphere during magnetic storms and leads to a decrease in the horizontal component of the magnetic field, with a maximum decrease at low latitudes. The Dst index is calculated as the average value of the perturbation of the horizontal component of the Earth's magnetic field strength per hour, counted from the quiet level, determined from the data of four low-latitude observatories evenly distributed along the geographic longitude. Dst is measured in nanotesla.

Another geomagnetic index predicted by us is the Kp index. It was officially introduced by Julius Bartels in 1949 [14]. Kp is a planetary index characterizing the global perturbation of the Earth's magnetic field in the three-hour time interval. The Kp index is determined as the average value of the perturbation levels of the two horizontal components of the geomagnetic field observed at 13 magnetic observatories located in the subauroral zone between 48° and 63° of geomagnetic latitude in the southern and northern hemispheres. The standardized values of the local K-indices of these 13 observatories are used to determine the planetary Kp index. Historically, the Kp index is measured once every three hours, the units are dimensionless, the minimum value of Kp is zero (no perturbations), the maximum value is 9 (very strong perturbations), each of the units is divided into three—1, 1+ (one and one third), 2– (one and two thirds), etc. [14].

Both the Dst and, in particular, the Kp index have a long-term observation history, which makes it possible to carry out statistical studies of the connection between geomagnetic activity and processes in the solar wind, interplanetary space, and the Earth's magnetosphere [15–20], most of which are based on the Burton formula [21], e.g., [22, 23].

A review of scientific foundations of magnetospheric space weather forecasting can be found in [24].

As for the prediction of the electron flux of the outer ERB, this is a separate task, solved by various methods in many countries.

A widely used forecast of the total flux per day (fluence) of the RE in the outer ERB is the forecast presented at the portal of the Space Weather Forecasting Center (Space Weather Prediction Center, http://www.swpc.noaa.gov/). This model is REFM—Relativistic Electron Forecast Model—http://www.swpc.noaa.gov/refm/ [25]. This forecast is based on the fact that the daily fluence values of electrons with an energy of >2 MeV, measured in a geosynchronous orbit, can be predicted a day in advance using a linear filter using the solar wind velocity as an input.

There are also a large number of other predictive models of the Earth's outer radiation belt created in other scientific groups, e.g. [26–29]. Separately mentioned should be NARMAX models [30], BAS Global Dynamic Radiation Belt Model (http://www.antarctica.ac.uk/bas_research/models/gdrbm/) [31], and the Salammb++ model, developed at the Aerospace Research Laboratory in Toulouse [32].

1.2. Use of Machine Learning for Space Weather Forecasting

Using machine learning (ML) methods allows one to establish relationships between the analyzed variables by approximating empirical dependencies.

The prediction of all the three above-mentioned physical quantities characterizing the state of the Earth's magnetosphere, carried out by ML methods, has a large number of similar features, such as, for example, the use of data on the solar wind and the interplanetary magnetic field as input parameters. Therefore, they are often considered together, as in [33].

In many countries, space weather portals operate, where neural network forecasting is used to predict Dst and Kp indices, for example—https://www.spaceweather.se/forecast/ in Sweden, https://eng.sepc.ac.cn/ in China [34].

At the same time, each of the predicted values has its own characteristics, for example, the three-hour step of the Kp index. So the current research on predicting each of the indices and the electron flux in the external ERB should be mentioned separately.

Dst index forecasting by ML methods has been studied in [35–43]. The prediction of the Kp index, taking into account its specifics, was considered in the following studies [44–50]. In the forecasting, various types of neural networks and adaptive methods are used. ML methods are used to predict the state of RE flux in the outer ERB in different orbits in [51–59].

The authors of this paper from the Laboratory of Adaptive Data Processing Methods at the Skobeltsyn Institute of Nuclear Physics of the Lomonosov Moscow State University, have also been working on the prediction of geomagnetic disturbances for quite a long time [60]. In relatively recent studies of the laboratory on forecasting of Dst index [61–63], Kp index within classification approach [64, 65], and RE flux on geostationary orbit [66–68], each pattern also

contained hourly averages of several main SW and IMF parameters and the predicted parameter itself for the last 24 h. This improved the quality of the forecast, but posed a new problem—the problem of selecting essential input features, giving rise to the study [69] and also to the current study.

2. PROBLEM STATEMENT

The Earth's magnetosphere is a complex dynamic system. This means that its state at each moment of time depends both on the current external influence from the Sun and on the prehistory of the magnetosphere itself. Therefore, forecasting requires the values of the parameters determining the state of the system at the previous moments of time (at the previous steps of the time series). This approach to forecasting leads to a strong increase in the dimension of input data, which complicates the work of machine learning algorithms and the analysis of the obtained results. In addition, the results become less interpretable.

The main idea is to solve the problem of time series analysis and predicting. Various methods can be employed to tackle the task of forecasting time series. The suggested approach allows predicting an event and determining of phenomena (a set of characteristics) that act as precursors or causes of the event. In this method we use machine learning algorithms that can be trained on different parts of the high dimensional dataset of variables. A key aspect of this algorithm is its capability to detect nonlinear relationships between the event and the phenomenon. Additionally, it can function in scenarios where intervention on the subject of study is not possible ("passive observation"), and the delay between the event and the phenomenon is not predetermined (only a range of acceptable delays is known). This method is universal and applicable to a lot of forecasting challenges in fields such as space physics, medicine, finance, and etc.

The purpose of this study is to adapt and apply the original 4-stage algorithm based on machine learning methods developed for analyzing multidimensional time series when solving problems of predicting certain events and identifying their precursors—phenomena represented by an unknown combination of parameter values describing the object.

In this research we apply this approach to forecast the following quantities: geomagnetic indices Kp and Dst, and the flux of relativistic electrons in the outer radiation belt of the Earth. Then we compare the results.

In addition, when forecasting time series, there is a task of comparing the quality with some baseline. Working with space weather forecasting, we use a trivial model (inertial forecast), which returns a predicted value equal to the last known one. Forecasts of such a model obviously do not have any practical meaning, but they make it possible to draw conclusions about the accuracy of the solution of the given task, and also allow one to demonstrate the justification for using more complex forecasting methods.

The solution of this problem helps us to improve the quality of forecasting geomagnetic disturbances, to decrease dimension of input data and to understand the most importance features and its lags.

It should also be noted that the specificity of space weather forecasting lies in the fact that statistical indicators characterizing the results of forecasting depend not only on the algorithms and techniques used, but also on the time intervals during which training and evaluation are performed. This is because the dynamics of the Earth's magnetosphere significantly depend on the current phase and other characteristics of the solar cycle. Therefore, it is difficult to compare the results obtained by different authors.

Moreover, this study aims not to obtain the highest possible forecast accuracy, but to develop an optimal forecasting methodology. For this reason, we do not compare our results with those of other authors, but rather compare the results of different forecasting procedures.

3. THE INPUT DATA

3.1. Initial Data

The values of the following quantities were used as input physical attributes (features):

1. Parameters of the interplanetary magnetic field (IMF) vector at the L1 Lagrange point of the system Sun–Earth in the GSM coordinate system: IMF components B_x, B_y, B_z, IMF modulus B_{magn} (nT).

2. Parameters of the solar wind (SW) at the same L1 point: velocity (km/s), density (cm^{-3}), temperature (K).

3. Geomagnetic indices: equatorial geomagnetic index Dst (nT), planetary geomagnetic index Kp (dimensionless).

4. Specially added random noise functions to test whether the system recognizes them as irrelevant for predicting the target variable.

The set also included four harmonic variables (two with a daily period and two with an annual period) to account for the Earth's rotation around its axis and around the Sun (time series embedding—taking into account the preceding values—was not used for these variables).

The SW and IMF data used in this paper were obtained on board the *Advanced Composition Explorer (ACE*) spacecraft, which has been in a quasi-stationary Lissajous orbit (so-called halo-orbit) near the Lagrangian point L1 of the Sun–Earth system since 1997. In the first approximation, ACE can be considered stationary relative to the Sun–Earth system, which minimizes the dependence of the data used on the spacecraft location. The values of the geomagnetic indexes were obtained from the site of the World Geomagnetism Data Center in Kyoto.

3.2. Data Preparation

Data from October 1997 to July 2023 were used. As mentioned above, apart from physical variables, 4 additional time parameters were introduced to take into account the phase of the day and the phase of the year.

- The training set was 1997–2015.
- The validation set was randomly generated as 20% of the training set. The validation set was used to avoid overfitting using early stopping option for gradient boosting.
- The test set was 2016–2023. This independent data was used to select the models at steps 2 and 3 of the algorithm, as well as to estimate final quality of solving our problem.
- The forecast horizon was selected as 3 h.

The study was performed on data with a time resolution of 1 h. Linear interpolation between two known values was used to fill gaps of up to 12 h long, larger gaps were removed from the dataset.

4. ALGORITHM DESCRIPTION

The algorithm lets us adaptively select both physical input features and specific delay values while taking into account the history of each physical feature within the topological embedding of its corresponding time series. Such selection can provide a better understanding of the processes occurring in the object under study. In this study, to build the forecasting models we used gradient boosting ML algorithm (XGBoost implementation, https://xgboost.ai/). The general scheme of the 4-stage algorithm includes the following steps:

1. Selection of the most significant physical attributes (variables) among those that, in the opinion of the researcher, can affect the predicted target value. The current implementation uses an iterative approach for this purpose. In this approach, the system estimates the correlation (Pearson/Spearman) between the input feature and its delays and the predicted variable on the training set. Then, based on a given threshold, a fraction of variables is selected to be used in the next steps.

2. Selection of the range of delays used. The input feature sets under consideration were created as follows. Set 0 consisted of the currently selected input variables. Set 1 contained all input variables from set 0, as well as all these variables with a delay of 1 time step. Set 2 included all input variables from set 1 as well as all these variables with a delay of 2 time steps; and so on up to a limit defined by the researcher. The machine learning model is trained on each dataset created within this loop and its quality is evaluated on the test dataset. The cycle stops when, according to a given criterion, increasing the delay range no longer results in a significant improvement in prediction accuracy.

3. Selection of the most important input features from the obtained feature space limited at the first two stages. For this stage, standard approaches to assessing the importance of input features can be used. In this study, we used permutation importance evaluated on the test set.

4. Hyperparameter tuning and comparison with reference models.

5. RESULTS

Let's consider the results at every step of the algorithm.

5.1. First Step

Here we present the main results we obtained at the first stage.

1. **Kp results**.

   The following physical variables were selected in the first step:

   (a) SW parameters (velocity, density, temperature).

(b) IMF parameters (B_z, $Bmagn$).

(c) Dst and Kp indices.

Figure 1 is an example of results of this step. The plot shows that changing velocity of solar wind has impact on changing the target variable (Kp index) at least in the fifty hours range.

2. **Dst results**

In case of analysing Dst-index, the first-step feature set looks the same.

(a) SW parameters (velocity, density, temperature)).

(b) IMF parameters (B_z, B_{magn}).

(c) Dst and Kp indices.

Here, in Fig. 2, we can see that z-component of IMF has good correlation with the target variable at small time lags.

3. **$E > 2$ MeV results**

Selected features for electron flux forecasting:

(a) SW parameters (velocity, density, temperature).

(b) IMF parameters (B_z, B_{magn}).

(c) Dst index.

(d) Electron flux $E > 2$ MeV.

In Fig. 3, a demonstration of a badly correlated feature is shown.

5.2. Second Step

In the second step, the system made a search for the optimal set consisting of the values of the physical variables obtained at the first step at the current moment in time and of their values at several preceding hours. For each of the target variables, it determined the number of delays that should be taken into account (optimal embedding depth). The models were trained on the training set, and the R^2 score was evaluated on the test set.

Figure 4 shows that the amount of lags to get the best quality of forecasting for Kp index is 4 h. According to Figs. 5 and 6, the amount of lags to get the best quality of forecasting for Dst index and electron flux is about 1 day.

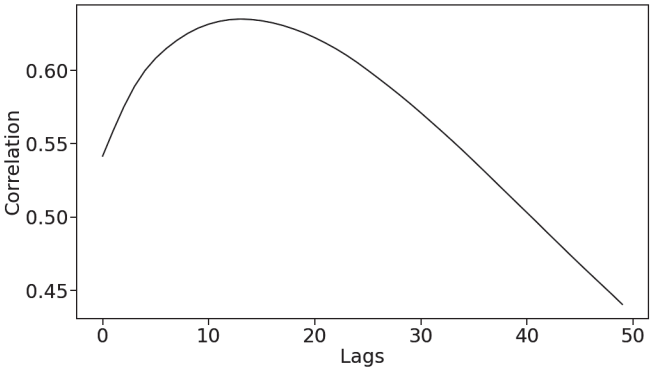

Fig. 1. Correlation coefficient between Kp index and solar wind velocity vs time lag.

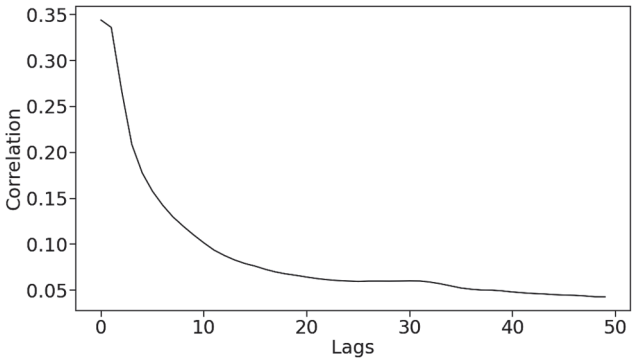

Fig. 2. Correlation coefficient between Dst index and z-component of IMF vs time lag.

5.3. Third Step

In the third step, the selection of the most important input features was performed in the space obtained in the first two steps. In this study, *permutation_importance* from the *sklearn* library was used as the selection algorithm. The permutation importance is defined to be the difference between the baseline metric and the metric from permutating the feature columns, where the metric was the coefficient of determination R^2 calculated on test set.

The determined importance of the features is displayed in Fig. 7 for Kp, in Fig. 8 for Dst, and in Fig. 9 for the electron flux.

Table 1. Quality metrics of the forecasting 3 h ahead (R^2 on the test set)

	Kp	Dst	E
Gradient boosting	0.725	0.855	0.854
Linear regression	0.711	0.833	0.829
Trivial model	0.549	0.733	0.726

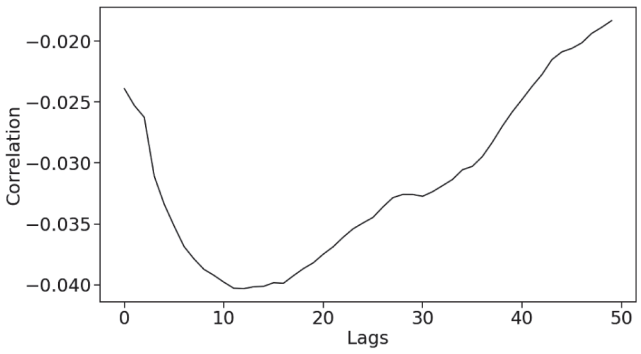

Fig. 3. Correlation coefficient between $E > 2$ MeV electron flux and z-component of the IMF vs time lag.

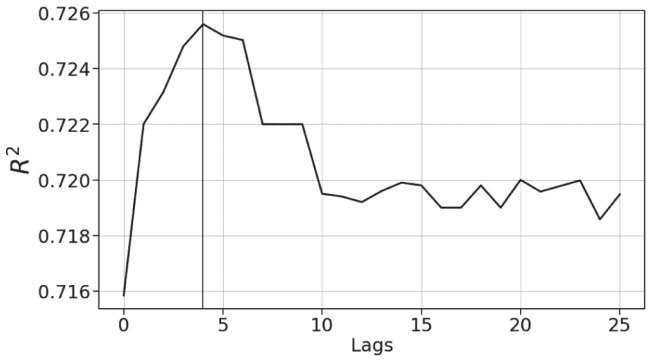

Fig. 4. The dependence of the R^2 test set score of the forecast for Kp index on the number of lags.

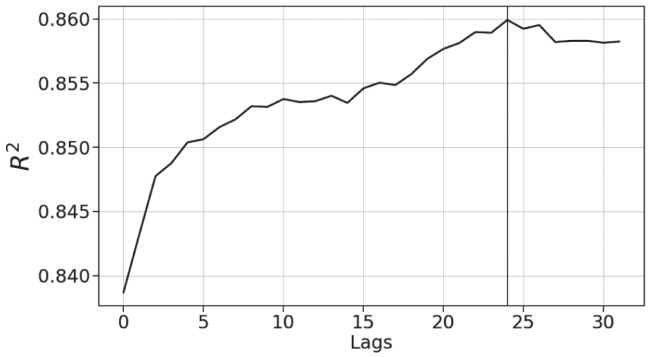

Fig. 5. The dependence of the R^2 test set score of the forecast for Dst index on the number of lags.

5.4. Fourth Step

Finally, we fine-tuned the gradient boosting models applied to the set of input features selected at the first three steps of the algorithm by grid search in the space of the parameters, and compared it with reference models. The grid search was based on the training set with cross validation.

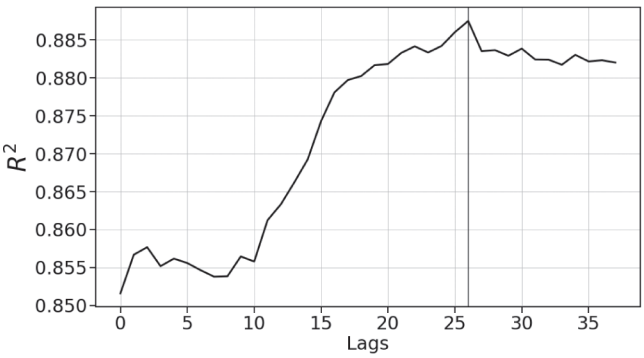

Fig. 6. The dependence of the R^2 test set score of the forecast for $E > 2$ MeV electron flux on the number of lags.

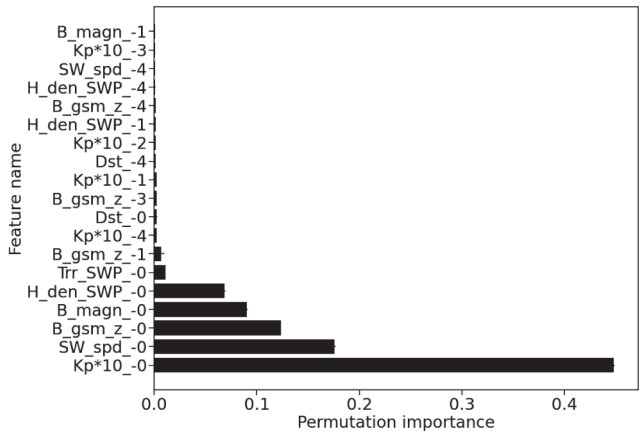

Fig. 7. Feature importance for Kp-index (ΔR^2 on the test set).

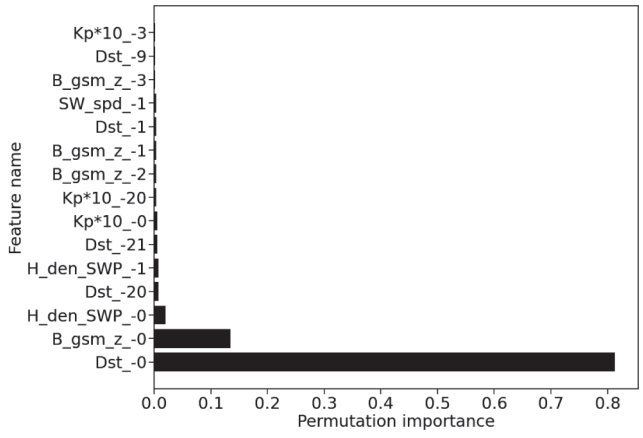

Fig. 8. Feature importance for Dst-index (ΔR^2 on the test set).

As reference models, we used the trivial inertial forecast (for which the predicted value is set equal

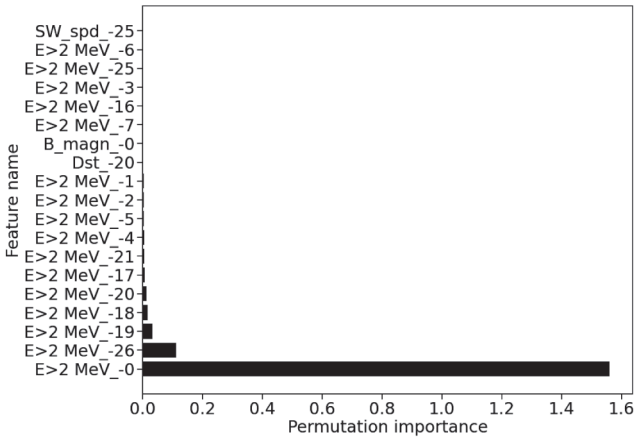

Fig. 9. Feature importance for $E > 2$ MeV electron flux (ΔR^2 on the test set).

to the last known value of the target variable at the forecasting moment) and the linear regression model with L2 regularization. The results are set together in Table 1.

It should be noted that as the test set was used to select the models at steps 2 and 3 of the algorithm, the test set is not completely and independent one, and the statistics on the test set provided in Table 1 may be somewhat overvalued. However, this does not affect the main conclusions regarding comparison of the algorithms and the selection of the most significant input features.

6. CONCLUSIONS

1. The application of the 4-step algorithm for predicting the Kp and Dst indices and for flux of electrons with energies above 2 MeV, was performed for prediction 3 h ahead.

2. From Table 1 we can see that the Gradient Boosting algorithm deals with all the problems better than linear regression with L2 regularization. Machine learning algorithms were also compared with the trivial model. Trivial model (inertial forecast) returns the predicted value that is equal to the last known value. The experiment shows, that both tested machine learning algorithms perform better than the trivial model.

3. The algorithm resulted in the selection of the following physical features with the following most important delays (lags):

   - Kp-index
     (a) SW velocity (0, 1, 2, 4), density (0, 1, 2, 3, 4), temperature (0, 3).
     (b) Kp-index (0, 1, 2, 3, 4), Dst-index (0, 1, 2, 3, 4).
     (c) IMF modulus B_{magn} (0, 1, 3, 4), IMF component B_z (0, 1, 2, 3, 4).
   - Dst-index
     (a) SW velocity (0, 1, 2, 4), density (0, 1).
     (b) Kp-index (0, 3, 20), Dst-index (0, 1, 9, 20, 21).
     (c) IMF component B_z (0, 1, 2, 3).
   - $E > 2$ MeV
     (a) SW velocity (25).
     (b) IMF Modulus B_{magn} (0).
     (c) Electron flux (0–26).

4. Future study should include evaluation of the models on yet another independent data set (e.g., 2024–2025).

FUNDING

This study was supported by the Russian Science Foundation, project no 23-21-00237, https://rscf.ru/en/project/23-21-00237/.

CONFLICT OF INTEREST

The authors of this work declare that they have no conflicts of interest.

REFERENCES

1. R. M. McGranaghan, E. Camporeale, M. Georgoulis, and A. Anastasiadis, J. Space Weather Space Clim. **11**, 50 (2021). https://doi.org/10.1051/swsc/2021037
2. I. A. Daglis, *Space Storms and Space Weather Hazards*, NATO Science Series II: Mathematics, Physics and Chemistry, Vol. 38 (Kluwer, Dordrecht, 2001). https://doi.org/10.1007/978-94-010-0983-6
3. K. Kudela, J. Phys.: Conf. Ser. **409**, 012017 (2013). https://doi.org/10.1088/1742-6596/409/1/012017
4. R. H. W. Friedel, G. D. Reeves, and T. Obara, J. Atmos. Sol.-Terr. Phys. **64**, 265 (2002). https://doi.org/10.1016/s1364-6826(01)00088-8
5. G. D. Reeves, K. L. McAdams, R. H. W. Friedel, and T. P. O'brien, Geophys. Res. Lett. **30**, 1529 (2003). https://doi.org/10.1029/2002gl016513
6. D. G. Cole, Space Sci. Rev. **107**, 295 (2003). https://doi.org/10.1023/A:1025500513499
7. V. B. Belakhovsky, V. A. Pilipenko, Ya. A. Sakharov, and V. N. Selivanov, Bull. Russ. Acad. Sci.: Phys. **87**, 236 (2023). https://doi.org/10.3103/s1062873822700988

8. Q. Qiu, J. A. Fleeman, and D. R. Ball, IEEE Electrif. Mag. **3** (4), 22 (2015). https://doi.org/10.1109/mele.2015.2480615
9. L. L. Lazutin, *Global and Polar Magnetic Storms* (Moskovskii Gosudarstvennyi Universitet, Moscow, 2012).
10. B. M. Vladimirsky and N. A. Temuryants, *The Influence of Solar Activity on the Biosphere-Noosphere* (IIUEPS, Moscow, 2000).
11. D. L. Turner, Yu. Shprits, M. Hartinger, and V. Angelopoulos, Nat. Phys. **8**, 208 (2012). https://doi.org/10.1038/nphys2185
12. I. N. Myagkova, Yu. S. Shugay, I. S. Veselovsky, and O. S. Yakovchouk, Sol. Syst. Res. **47**, 127 (2013). https://doi.org/10.1134/s0038094613020068
13. M. Sugiura, Annu. Int. Geophys. **35**, 9 (1964).
14. J. R. Bartels, IATME Bull., No. 12b, 97 (1949). https://doi.org/10.25577/xkjt-w404
15. H. A. Elliott, J. Jahn, and D. J. McComas, Space Weather **11**, 339 (2013). https://doi.org/10.1002/swe.20053
16. R. L. McPherron and P. O'Brien, in *Space Weather*, Ed. by P. Song, H. J. Singer, and G. L. Siscoe, Geophysical Monograph Series (American Geophysical Union, Washington, DC, 2001), p. 339. https://doi.org/10.1029/gm125p0339
17. T. P. O'Brien and R. L. McPherron, J. Atmos. Sol.-Terr. Phys. **62**, 1295 (2000). https://doi.org/10.1016/s1364-6826(00)00072-9
18. G. Pallocchia, E. Amata, G. Consolini, M. F. Marcucci, and I. Bertello, Ann. Geophys. **24**, 989 (2006). https://doi.org/10.5194/angeo-24-989-2006
19. T. V. Podladchikova and A. A. Petrukovich, Space Weather **10**, 7001 (2012). https://doi.org/10.1029/2012sw000786
20. S. Patra, E. Spencer, W. Horton, and J. Sojka, J. Geophys. Res.: Space Phys. **116**, A02212 (2011). https://doi.org/10.1029/2010ja015824
21. R. K. Burton, R. L. McPherron, and C. T. Russell, J. Geophys. Res. **80**, 4204 (1975). https://doi.org/10.1029/ja080i031p04204
22. M. Temerin and X. Li, J. Geophys. Res.: Space Phys. **107**, SMP31 (2002). https://doi.org/10.1029/2001ja007532
23. M. Temerin and X. Li, J. Geophys. Res.: Space Phys. **111**, A04221 (2006). https://doi.org/10.1029/2005ja011257
24. J. P. Eastwood, R. Nakamura, L. Turc, L. Mejnertsen, and M. Hesse, Space Sci. Rev. **212**, 1221 (2017). https://doi.org/10.1007/s11214-017-0399-8
25. D. N. Baker, R. L. McPherron, T. E. Cayton, and R. W. Klebesadel, J. Geophys. Res.: Space Phys. **95**, 15133 (1990). https://doi.org/10.1029/JA095iA09p15133
26. W. Lyatsky and G. V. Khazanov, Geophys. Res. Lett. **35**, L15108 (2008). https://doi.org/10.1029/2008gl034688
27. M. H. Denton, M. G. Henderson, V. K. Jordanova, M. F. Thomsen, J. E. Borovsky, J. Woodroffe, D. P. Hartley, and D. Pitchford, Space Weather **14**, 511 (2016). https://doi.org/10.1002/2016sw001409
28. M. A. Balikhin, J. V. Rodriguez, R. J. Boynton, S. N. Walker, H. Aryan, D. G. Sibeck, and S. A. Billings, Space Weather **14**, 22 (2016). https://doi.org/10.1002/2015sw001303
29. A. Potapov, L. Ryzhakova, and B. Tsegmed, Acta Astronaut. **126**, 47 (2016). https://doi.org/10.1016/j.actaastro.2016.04.017
30. M. A. Balikhin, R. J. Boynton, S. N. Walker, J. E. Borovsky, S. A. Billings, and H. L. Wei, Geophys. Res. Lett. **38**, L18105 (2011). https://doi.org/10.1029/2011gl048980
31. S. A. Glauert, R. B. Horne, and N. P. Meredith, J. Geophys. Res.: Space Phys. **119**, 268 (2014). https://doi.org/10.1002/2013ja019281
32. T. Beutier and D. Boscher, J. Geophys. Res.: Space Phys. **100**, 14853 (1995). https://doi.org/10.1029/94ja03066
33. P. Wintoft and M. Wik, Space Weather **16**, 1972 (2018). https://doi.org/10.1029/2018sw001994
34. S. Liu and J. Gong, Space Weather **13**, 599 (2015). https://doi.org/10.1002/2015sw001298
35. N. A. Barkhatov, N. S. Bellustin, A. E. Levitin, and S. Y. Sakharov, Radiophys. Quantum Electron. **43**, 347 (2000). https://doi.org/10.1007/bf02677150
36. J. Wu and H. Lundstedt, J. Geophys. Res.: Space Phys. **102**, 14255 (1997). https://doi.org/10.1029/97ja00975
37. M. V. Stepanova and P. Pérez, Geofísica Internacional **39**, 143 (2000). https://doi.org/10.22201/igeof.00167169p.2000.39.1.310
38. M. Revallo, F. Valach, P. Hejda, and J. Bochníček, Contrib. Geophys. Geod. **45**, 53 (2015). https://doi.org/10.1515/congeo-2015-0013
39. B. Xue and J. Gong, Chin. J. Space Sci. **26**, 183 (2006). https://doi.org/10.11728/cjss2006.03.183
40. J. A. Lazzús, P. Vega, P. Rojas, and I. Salfate, Space Weather **15**, 1068 (2017). https://doi.org/10.1002/2017sw001608
41. M. A. Gruet, M. Chandorkar, A. Sicard, and E. Camporeale, Space Weather **16**, 1882 (2018). https://doi.org/10.1029/2018sw001898
42. A. Lethy, M. A. El-eraki, A. Samy, and H. A. Deebes, Space Weather **16**, 1277 (2018). https://doi.org/10.1029/2018sw001863
43. W. Park, J. Lee, K.-C. Kim, J. Lee, K. Park, Yu. Miyashita, J. Sohn, J. Park, Y.-S. Kwak, J. Hwang, A. Frias, J. Kim, and Yu. Yi, J. Space Weather Space Clim. **11**, 38 (2021). https://doi.org/10.1051/swsc/2021021

44. F. Boberg, P. Wintoft, and H. Lundstedt, Phys. Chem. Earth, Part C: Sol., Terr. Planet. Sci. **25**, 275 (2000). https://doi.org/10.1016/s1464-1917(00)00016-7
45. E. Ji, Y.-J. Moon, J. Park, J. Lee, and D.-H. Lee, J. Geophys. Res.: Space Phys. **118**, 5109 (2013). https://doi.org/10.1002/jgra.50500
46. Ya. Tan, Q. Hu, Zh. Wang, and Q. Zhong, Space Weather **16**, 406 (2018). https://doi.org/10.1002/2017sw001764
47. S. Wing, J. R. Johnson, J. Jen, C.-I. Meng, D. G. Sibeck, K. Bechtold, J. Freeman, K. Costello, M. Balikhin, and K. Takahashi, J. Geophys. Res.: Space Phys. **110**, A04203 (2005). https://doi.org/10.1029/2004ja010500
48. R. Bala and P. Reiff, Space Weather **10**, S06001 (2012). https://doi.org/10.1029/2012sw000779
49. R. Bala and P. Reiff, Space Weather **12**, 417 (2014). https://doi.org/10.1002/2014sw001075
50. J. Wang, Q. Zhong, S. Liu, J. Miao, F. Liu, Zh. Li, and W. Tang, Space Weather **13**, 831 (2015). https://doi.org/10.1002/2015sw001251
51. H. C. Koons and D. J. Gorney, J. Geophys. Res. Space Phys **96**, 5549 (1991). https://doi.org/10.1029/90JA02380
52. M. Fukata, S. Taguchi, T. Okuzawa, and T. Obara, Ann. Geophys. **20**, 947 (2002). https://doi.org/10.5194/angeo-20-947-2002
53. A. G. Ling, G. P. Ginet, R. V. Hilmer, and K. L. Perry, Space Weather **8**, S09003 (2010). https://doi.org/10.1029/2010sw000576
54. K. Kitamura, Y. Nakamura, M. Tokumitsu, Y. Ishida, and S. Watari, Artif. Life Rob. **16**, 389 (2011). https://doi.org/10.1007/s10015-011-0957-1
55. D.-K. Shin, D.-Y. Lee, K.-C. Kim, J. Hwang, and J. Kim, Space Weather **14**, 313 (2016). https://doi.org/10.1002/2015sw001359
56. R. Pires de Lima, Yu. Chen, and Yo. Lin, Space Weather **18**, e2019SW002399 (2019). https://doi.org/10.1029/2019sw002399
57. X. Chu, D. Ma, J. Bortnik, W. K. Tobiska, A. Cruz, S. D. Bouwer, H. Zhao, Q. Ma, K. Zhang, D. N. Baker, X. Li, H. Spence, and G. Reeves, Space Weather **19**, e2021SW002808 (2021). https://doi.org/10.1029/2021sw002808
58. S. Killey, I. J. Rae, S. Chakraborty, A. W. Smith, S. N. Bentley, M. R. Bakrania, R. Wainwright, C. E. J. Watt, and J. K. Sandhu, RAS Techniques and Instruments **2**, 548 (2023). https://doi.org/10.1093/rasti/rzad035
59. E. Botek, V. Pierrard, and A. Winant, Space Weather **21**, e2023SW003466 (2023). https://doi.org/10.1029/2023sw003466
60. S. A. Dolenko, Yu. V. Orlov, I. G. Persiantsev, and Ju. S. Shugai, in *Artificial Neural Networks: Formal Models and Their Applications—ICANN 2005*, Ed. by W. Duch, J. Kacprzyk, E. Oja, and S. Zadrożny, Lecture Notes in Computer Science, Vol. 3697 (Springer, Berlin, 2005), p. 527. https://doi.org/10.1007/11550907_83
61. A. O. Efitorov, I. N. Myagkova, V. R. Shirokii, and S. A. Dolenko, Cosmic Res. **56**, 434 (2018). https://doi.org/10.1134/s0010952518060035
62. I. Myagkova, V. Shiroky, and S. Dolenko, E3S Web Conf. **20**, 02011 (2017). https://doi.org/10.1051/e3sconf/20172002011
63. I. N. Myagkova, V. R. Shirokii, R. D. Vladimirov, O. G. Barinov, and S. A. Dolenko, Russ. Meteorol. Hydrol. **46**, 157 (2021). https://doi.org/10.3103/s1068373921030031
64. I. M. Gadzhiev, I. V. Isaev, O. G. Barinov, S. A. Dolenko, and I. N. Myagkova, Moscow Univ. Phys. Bull. **78**, S96 (2023). https://doi.org/10.3103/s002713492307007x
65. I. M. Gadzhiev, O. G. Barinov, I. N. Myagkova, and S. A. Dolenko, Geomagn. Aeron. **64**, 415 (2024). https://doi.org/10.1134/S0016793224600140
66. I. N. Myagkova, S. A. Dolenko, A. O. Efitorov, V. R. Shirokii, and N. S. Sentemova, Geomagn. Aeron. (Engl. Transl.) **57**, 8 (2017). https://doi.org/10.1134/s0016793217010108
67. I. N. Myagkova, V. R. Shirokii, Yu. S. Shugai, O. G. Barinov, R. D. Vladimirov, and S. A. Dolenko, Russ. Meteorol. Hydrol. **46**, 163 (2021). https://doi.org/10.3103/s1068373921030043
68. V. Kalegaev, K. Kaportseva, I. Myagkova, Yu. Shugay, N. Vlasova, W. Barinova, S. Dolenko, V. Eremeev, and A. Shiryaev, Adv. Space Res. **72**, 5376 (2023). https://doi.org/10.1016/j.asr.2022.08.033
69. R. D. Vladimirov, V. R. Shirokiy, I. N. Myagkova, O. G. Barinov, and S. A. Dolenko, Geomagn. Aeron. (Engl. Transl.) **63**, 161 (2023). https://doi.org/10.1134/s0016793222600795